NB-IoT for Direct-to-Satellite Communications: Performance Modeling and Evaluation

Enrico Testi*, Riccardo Marini†, Gianni Pasolini*, Enrico Paolini*
*DEI, University of Bologna / WiLab, CNIT, Bologna, Italy, Email: {enrico.testi, gianni.pasolini, e.paolini}@unibo.it
†WiLab, CNIT, Bologna, Italy, Email: riccardo.marini@wilab.cnit.it

***Abstract*—The rapid growth in Internet of Things (IoT) applications has driven demand for ubiquitous connectivity, reaching beyond terrestrial networks to include satellite communication solutions. This paper investigates the application of Narrowband IoT (NB-IoT) within Non-Terrestrial Networks (NTNs), specifically focusing on direct-to-satellite (DtS) communications for IoT in Low Earth Orbit (LEO) constellations. This study first provides an overview of NB-IoT's protocol adaptations required for NTN use, followed by the introduction of an analytical model for network throughput that incorporates the dependence on key system parameters, such as satellite velocity, spot size, and ground node density. Our results analyze key NB-IoT parameters affecting network performance, providing insights on configuration strategies to optimize connectivity for remote IoT deployments via LEO satellites. The findings contribute to understanding the feasibility of NB-IoT for DtS communication, highlighting practical considerations and performance trade-offs for deploying IoT over NTN.**

I. Introduction

In recent years, low Earth orbit (LEO) satellite constellations have emerged as a cornerstone for extending Internet of Things (IoT) connectivity worldwide, attracting substantial interest from private industries, international standards bodies, and the academic community [1]–[3]. With the rapid evolution of communication networks towards beyond-5G and upcoming 6G technologies, new demands for connectivity are pushing systems to higher spectral efficiency, reduced latency, and increased global accessibility. To meet these demands, 6G networks are anticipated to adopt a multi-layered architecture that seamlessly integrates terrestrial and non-terrestrial network (NTN), providing a robust framework for diverse applications such as remote monitoring, connectivity for underserved areas, and global intelligent transportation systems [4]. Currently, the Third Generation Partnership Project (3GPP) is actively supporting Narrowband IoT (NB-IoT) standards for NTNs, while companies like Lacuna Space and EchoStar Mobile are pioneering proprietary low power wide area network (LPWAN) technologies to enhance direct-to-satellite IoT (DtS-IoT) communications [5]–[7].

Driven by the increasing interest of 3GPP in NTNs, several recent studies have analyzed the performance of NB-IoT and its alternatives in direct-to-satellite (DtS) communications. In [8], [9], a link-level performance evaluation of DtS communications from IoT devices on Earth is performed, without addressing network-level performance. In [10], the performance of NB-IoT is studied on a system-level perspective, in terms of access delay and access success probability under different network densities and configuration parameters. The authors in [10] propose an analytical model for the access success probability, assuming a system with a fixed number of active users, while [11] investigates link-level features and overall network performance for an agriculture use case via simulations. Extensive simulations to investigate network performance are performed in [12] as well.

The main contribution of this paper can be summarized as follows. First, we offer an overview of the NB-IoT protocol and how it can be used in an NTN scenario. Second, in contrast to prior works, we introduce an analytical model for network throughput that incorporates the dependence on key system parameters, such as satellite velocity, spot size, and ground node density. Notably, our model does not assume a fixed number of users, but instead considers a Poisson point process (PPP) for the distribution of devices on the ground. The model is then validated via extensive simulations. Finally, we carry out a network performance analysis via simulation investigating how the key NB-IoT-related parameters, e.g., the number of subcarriers and the random access window periodicity, impact the system performance, delineating a trade-off between reliability and scalability.

The remainder of the paper is organized as follows. Section II describes the NB-IoT protocol stack and its operations. Section III details the analytical network throughput model. Results are discussed in Section IV. Finally, Section V concludes the paper.

II. NB-IoT in a nutshell

A. NB-IoT Technology

NB-IoT is engineered to deliver efficient connectivity in cellular IoT scenarios, ensuring long battery life for a wide distribution of machine terminals. It supports many connections per cell and provides robust coverage, enabling connectivity in challenging environments like underground and indoor locations [13].

Introduced in Release 13 of the 3GPP specification documents, NB-IoT has emerged as a competitive alternative to existing LPWAN technologies such as LoRaWAN. It utilizes LTE standard numerology, adapted for low-cost machine type communication (MTC), accommodating a high density of devices per cell. NB-IoT retains key LTE mechanisms such as synchronization, radio access, resource definition, and assignment. However, modifications have been made to enhance

TABLE I
NB-IoT KEY PARAMETER VALUES

Parameters	Values
Bit Rate	up to 253.6kbit/s
Frequency Bands	[400, 2700] MHz
Physical Resource Block	180kHz
Link budget	up to 164dB
TX Range	up to 10 km

the link budget and significantly reduce energy consumption, complexity, and costs.

NB-IoT can operate in three distinct modes concerning spectrum usage: i) standalone mode, ii) within the guard bands of LTE carriers, or iii) in-band within LTE carriers. Similar to LTE, NB-IoT eNodeBs (eNBs) utilize orthogonal frequency division multiple access (OFDMA) in the downlink, while user equipments (UEs) employ single carrier frequency division multiple access (SC-FDMA) in the uplink. The modulation schemes are restricted to binary phase shift keying (BPSK) and quadrature phase shift keying (QPSK) to minimize complexity and improve the link budget. NB-IoT supports a nominal system bandwidth of 180 kHz, equivalent to one LTE physical resource block (PRB), in both uplink and downlink.

In the downlink, the frequency separation is fixed at 15 kHz, using the concept of PRBs. A PRB spans 12 subcarriers and 7 orthogonal frequency division multiplexing (OFDM) symbols, and a pair of PRBs form the smallest schedulable unit, known as a subframe, with a total duration of one millisecond. In the uplink, the resource grid consists of multiple subcarrier frequencies with a separation (Δf) of either 3.75 kHz or 15 kHz [14]. This leads to a number of available subcarriers B equal to 48 or 12, respectively. Time slots are 0.5 ms and 2 ms in duration for Δf = 15 kHz and Δf = 3.75 kHz. NB-IoT introduces resource elements (REs) and resource units (RUs), with REs representing the smallest time-frequency resource and RUs combining specific numbers of consecutive subcarriers and time slots.

Hybrid automatic repeat request (HARQ) is implemented by default in both uplink and downlink and, additionally, UEs (category NB1/NB2) implement power control in the uplink to reduce power consumption when feasible. Coverage enhancement is primarily achieved by employing repetitions to exploit time diversity, repeating transmissions multiple times, thus allowing the receiver to combine replicas. Repetitions increase energy and time consumption, so UEs are categorized into three coverage classes—Normal, Robust, and Extreme—based on the number of repetitions and configurations affecting coverage.

Table I summarizes key parameter values for NB-IoT.

B. NB-IoT Random Access Procedure

To elucidate NB-IoT procedures, we detail the operations in a frequency division duplexing (FDD) network [13]. Upon powering up, a UE initiates the cell search procedure, acquiring time and frequency synchronization with a cell, identifying it, and obtaining configuration information from periodically broadcast information blocks.

Once the required information is acquired, the UE attempts to establish a network connection by executing the random access (RA) procedure to gain access to a radio channel. The UE waits for a scheduled random access channel (RACH) window (or random access occasion (RAO)), which is scheduled with a periodicity of T_{RA}, and transmits a randomly selected preamble. The preamble consists of four groups of symbols, with carrier frequency changes for each group. Three narrowband physical random access channel (NPRACH) preamble formats are defined, offering trade-offs between on-air time and maximum communication range. Up to three periodic NPRACH windows can be configured per cell, each associated with a conditional entropy (CE) level and different preamble repetitions (1 to 128). The UE selects the coverage class based on reference signal received power (RSRP) estimation, network configuration, and previous unsuccessful RA attempts. The NPRACH transmission, often referred to as Message 1 (Msg1), is the first message in the RA procedure.

If multiple UEs select the same preamble, their transmissions overlap. The eNB schedules the RA Response (RAR or Msg2) via the narrowband physical downlink control channel (NPDCCH). The RAR is sent using the narrowband physical downlink shared channel (NPDSCH), allocating resources and specifying the modulation and coding scheme (MCS) and repetitions for the next uplink transmission for each received RA preamble. The UEs with the same preamble receive the same RAR and transmit Msg3, containing the buffer size report (BSR) and UE Contention Resolution Identity, using narrowband physical uplink shared channel (NPUSCH) resources, then await the radio resource control (RRC) connection setup (Msg4), again scheduled via NPDCCH. Msg4 grants resources for data transmission and resolves possible collisions. This procedure repeats each time an unconnected UE needs to access radio resources to transmit data.

Early data transmission (EDT) is a key enhancement introduced in NB-IoT to optimize energy consumption and reduce latency, primarily for devices with sporadic and low-rate uplink data transmissions. This mechanism allows devices to transmit small amounts of data during the RACH procedure, bypassing the traditional multi-step connection establishment process, and letting the device transmit transmit its payload earlier, specifically appending it to Msg3. This reduces the overall signaling overhead and latency. However, EDT is primarily designed for small payloads. The maximum data size that can be transmitted depends on the network configuration and can vary based on system load and device category. As specific in [15], to enable EDT the packet requires 23 bytes of overhead overall and, in general, the transport block size (TBS) in this case cannot exceed 1000 bits (operator-specific configurations that may further reduce this limit).

C. NB-IoT for NTN Scenarios

The integration of NTN into the terrestrial system architecture has been acknowledged by 3GPP, incorporating NTN into

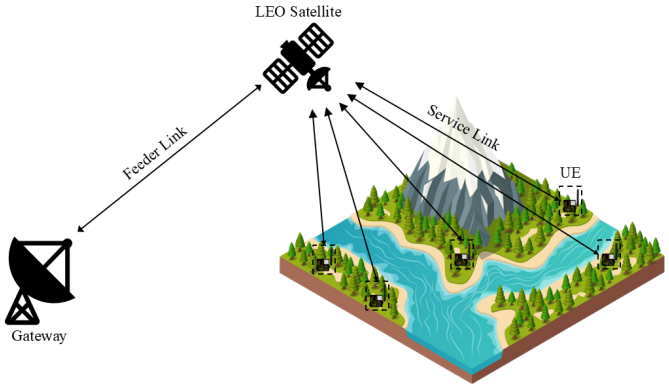

Fig. 1. Satellite IoT scenario in which a set of active devices deployed in remote areas perform DtS uplink transmissions.

New Radio (NR) beginning with Rel. 17. Concurrently, in 2021, 3GPP initiated a feasibility study to explore the adaptation of the NB-IoT air interface for satellite communication, marking the start of NB-IoT support for NTN. Technical Report TR 36.763 [16] outlines the required adaptations and assesses the performance of NB-IoT over NTN channels.

The reference architecture incorporates NTN UEs, satellites, and Gateways, as outlined in [16] and depicted in Figure 1. NTN UEs communicate with satellites via the service link, establishing a connection with a single satellite from the constellation during its visibility period. When a subsequent satellite from the same orbit enters the coverage area of the NTN UE, configuration procedures proceed in a stateless manner. Satellites and Gateways, in turn, connect over the feeder link, which may involve a time-shifted interaction if the Gateway is located in a different geographical area. In the following, we assume the full evolved packet system (EPS) protocol stack on the satellite and a network architecture that decouples the service link from the feeder link, enabling asynchronous data transmission over the service link even when feeder-link availability to the Gateway is intermittent. We also assume UEs to use EDT so that signalling required for communication is reduced.

III. NB-IoT Throughput Analysis for DtS Uplink

We analyze the uplink communication of a non-terrestrial IoT system in which ground-based devices compete to transmit packets to a LEO satellite during its pass. The satellite moves, parallel to the ground, with a constant velocity $\boldsymbol{v}$ such that $v = |\boldsymbol{v}|$. We assume that all devices on ground are synchronous with the satellite, e.g., through a beacon signal periodically broadcast by the satellite. Additionally, the satellite periodically broadcasts its orbital data to the nodes, allowing each device to be aware of the start and end of its visibility window and to synchronize its uplink attempts accordingly. At every pass, each active node attempts transmission of one message following the uplink operation sequence detailed in Section II-B. Once a device enters the satellite's visibility range, it waits for the next available RACH window to attempt an uplink transmission.

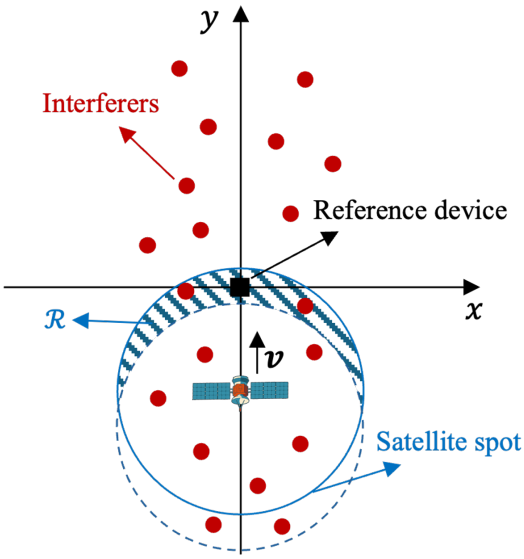

Fig. 2. Illustration of the adopted reference coordinate system and the satellite's trajectory along the y-axis. The reference device is positioned at the origin, while interfering devices are distributed across $\mathbb{R}^2$ according to a PPP. The shaded region, denoted as $\mathcal{R}$, represents the area covered by the satellite between two consecutive RACH windows.

In the event of a failed transmission, the device enters a backlog state and reattempts transmission in the subsequent RACH window. This retry process continues until the device successfully transmits its packet or exits the satellite's visibility range. The access protocol is uncoordinated, meaning each device operates independently, without coordination with other devices. Throughout the analysis, we neglect the Earth's curvature, modeling the ground as a plane, and we assume that the satellite spot shape does not change over time. The analysis focuses on a single satellite pass, adopting a Cartesian coordinate system in which the satellite's velocity, $\boldsymbol{v}$, aligns with the y axis, as depicted in Figure 2.

The transmitting devices are assumed to be scattered in the x–y plane according to a PPP with spatial density λ, such that their number in a measurable region is a Poisson distributed random variable. We denote by $\mathcal{R}$ the region swept by the satellite spot between two consecutive RACH windows, and by $A_{\mathcal{R}}$ its area. We also denote a device as "fresh" if it has entered the satellite's coverage area after the beginning of the previous RACH window, and is attempting transmission for the first time during the current RACH window. It can be easily seen that the number of fresh devices in a RACH window, F, is a Poisson random variable with mean value $\bar{F}$, which depends on the nodes' density on ground, λ, and on the region $\mathcal{R}$ spanned by the satellite between two consecutive RACH windows. Thus, the average number of fresh arrivals during a RACH window can be expressed as:

$$\bar{F} = \lambda A_{\mathcal{R}} = \rho T_{\text{RA}} \tag{1}$$

where ρ is the rate of devices entering the satellite spot between two consecutive RACH windows, and T_{RA} is the time between the beginning of two consecutive RACH windows. While the

first part of (1) relates the fresh arrivals with the spatial PPP, which regulates the distribution of devices on ground, the second part of the equation relates the fresh arrivals with the time process regulating the rate of devices entering the satellite spot between two consecutive RACH windows. The rate ρ can thus be obtained as a function of λ, $A_{\mathcal{R}}$, and T_{RA}. For a circular satellite spot with radius L, the area covered by the spot between two consecutive RACH windows can be determined by first calculating the intersection area of two overlapping circles—representing the spot's position at the start and end of the RACH window—and then subtracting this intersection area from the total spot area. Thus, we have

$$A_{\mathcal{R}} = L^2 \left(\pi - 2\cos^{-1}\left(\frac{vT_{\text{RA}}}{2L} \right) \right) + \frac{vT_{\text{RA}}}{2} \sqrt{4L^2 - (vT_{\text{RA}})^2}. \tag{2}$$

We define a transmission attempt during a RACH procedure as unsuccessful if a collision occurs in the Msg3 message. Let us now denote by b the number of backlogged devices attempting retransmission during a RACH window, i.e., devices whose packet transmission was unsuccessful in the previous RACH window. The average traffic load of the system in a generic RACH window can be expressed as

$$G(b) = \bar{F} + b = \rho T_{\text{RA}} + b. \tag{3}$$

Let us denote by X the random variable (r.v.) representing the number of packets correctly received in a RACH, with $X \in \{0, 1, 2, \ldots, B\}$. The system throughput is a function of the number of packets that are being retransmitted and is

$$S(b) = \sum_{n=1}^{B} nP(X = n|b). \tag{4}$$

Given the number of fresh arrivals, $F = f$, the conditional probability $P(X = n|b)$ can be developed as

$$P(X = n|b) = \sum_{f=0}^{\infty} P(X = n|b, f)P(F = f). \tag{5}$$

Incorporating (5) into (4) yields

$$S(b) = \sum_{f=0}^{\infty} P(F = f) \sum_{n=1}^{B} nP(X = n|b, f). \tag{6}$$

Now, we note that $P(X = n|b, f)$ can be viewed as the number of ways of allocating $f + b$ distinguishable packets into B distinguishable frequency channels, such that n channels receive exactly 1 packet, divided by all the possible combinations. This can be expressed mathematically as

$$P(X = n|b, f) = \binom{f+b}{n} \frac{B!}{(B-n)!B^{f+b}} V \tag{7}$$

where V denotes the number of ways of allocating $f + b - n$ distinguishable packets to $B - n$ distinguishable channels such that no channel takes exactly 1 packet. This can be calculated by extracting the coefficient of degree $f+b-n$ of the exponential generating function (EGF) for a channel that does not receive exactly 1 packet, i.e.,

$$\mathsf{EGF}_V(z) = \sum_{k=0}^{\infty} \frac{z^k}{k!} - z = e^z - z. \tag{8}$$

Thus, V can be expressed as

$$\begin{aligned} V &= (f+b-n)!\,\text{coeff}\left[(e^z - z)^{B-n}, z^{f+b-n}\right] \\ &= (f+b-n)! \sum_{i=0}^{B-n} \binom{B-n}{i} e^{iz} (-1)^{B-n-i} z^{B-n-i} \\ &= (f+b-n)! \left((-1)^{B-n} z^{B-n} + \sum_{i=1}^{B-n} \binom{B-n}{i} \right. \\ &\qquad \left. \times (-1)^{B-n-i} z^{B-n-i} \sum_{t=0}^{\infty} \frac{(iz)^t}{t!} \right). \end{aligned} \tag{9}$$

Let us now write $t = b + f - B + i$, which is possible if and only if $i \geq B - (b + f)$, such that the expression of V can be further simplified as

$$\begin{aligned} V = (f+b-n)! \Bigg(&(-1)^{B-n} \mathbf{1}_{\{f+b=B\}} \\ &+ \sum_{i=\max(1, B-(b+f))}^{B-n} \binom{B-n}{i} (-1)^{B-n-i} \frac{i^{i+b+f-B}}{(i+b+f-B)!} \Bigg) \end{aligned} \tag{10}$$

where $\mathbf{1}_{\{\mathcal{C}\}}$ is the indicator function returning 1 if condition $\mathcal{C}$ is verified, and 0 otherwise. Incorporating (7) and (9) into (4) yields (11).

IV. Numerical Results

In this section, a NB-IoT DtS uplink simulator is first used to compare the performance of this technology under different parameter configurations, examining the trade-off between reliability and scalability. Then, the validity of the proposed analytical model is assessed.

The satellite orbits at an altitude of 600 km above the Earth's surface, traveling at a velocity $v = 7.5\,\text{km/s}$. We assume a circular satellite coverage area, i.e., a circular spot shape, with a radius of $L = 420.124\,\text{km}$, determined based on a minimum elevation angle of $\epsilon = 55°$ for effective device-satellite communication. For NB-IoT, the number of available subcarriers, denoted by B, can be either 12 or 48, corresponding to subcarrier spacings of 15 kHz or 3.75 kHz, respectively. The duration of the RACH window—the interval between two consecutive RACH opportunities—is set at either $T_{\text{RA}} = 320\,\text{ms}$, $T_{\text{RA}} = 640\,\text{ms}$, or $T_{\text{RA}} = 1280\,\text{ms}$. The complete list of simulation parameters is given in Table II.

A. NB-IoT DtS Uplink Simulator

The performance of NB-IoT in DtS communication scenarios is evaluated through a Monte Carlo simulation framework. This simulation tool models random channel access by ground-based nodes that attempt to transmit messages to a passing

$$S(b) = \frac{B! e^{-\rho T_{\mathrm{RA}}}}{B^b} \sum_{f=0}^{\infty} \frac{(f+b)!}{f!} \left(\frac{\rho T_{\mathrm{RA}}}{B}\right)^f \sum_{n=1}^{\min(U, f+b)} \frac{1}{(n-1)!(B-n)!} \tag{11}$$
$$\times \left((-1)^{B-n} \mathbf{1}_{\{f+b=B\}} + \sum_{i=\max(1, B-(b+f))}^{B-n} \binom{B-n}{i} (-1)^{B-n-i} \frac{i^{i+b+f-B}}{(i+b+f-B)!} \right).$$

TABLE II
SIMULATION PARAMETERS

Parameters	**Values**
Satellite orbit height	600 km
Satellite velocity	7.5 km/s
Circular spot shape radius (L)	420.124 km
Minimum elevation angle	55°
NB-IoT subcarriers	12, 48
NB-IoT subcarrier spacings	15 kHz, 3.75 kHz
RACH window periodicity (T_{RA})	320 ms, 640 ms, 1280 ms

satellite using the NB-IoT protocol, as detailed in Section II-C.[1] We introduce a reference UE positioned at the origin of the reference coordinate system, depicted in Figure 2. For each Monte Carlo iteration, the number of interfering nodes within region $\mathcal{R}$, spanned by the satellite between two consecutive RACH windows, is sampled from a Poisson distribution with density parameter λ, after which the interfering nodes are uniformly distributed within $\mathcal{R}$. Let S denote the event that the reference UE's message is successfully received by the satellite during a pass. This occurs if during the satellite's pass there exists one RACH window in which the Msg3 transmitted by the reference device does not experience a collision. We define $P(\mathsf{S})$ as the probability of this successful transmission, i.e., the "success probability".

To mitigate edge effects and ensure stable system behavior upon reaching the reference UE, we initiate the simulation with the satellite pass over an empty region (i.e., a region populated solely by interfering devices), allowing it to progress through N_{pre} RACH windows before reaching the reference device's position. This setup enables the system to stabilize, reaching either a steady or congested state—depending on the number of devices contending for uplink access—by the time the satellite enters the reference device's vicinity. This approach prevents the analysis of network performance during the initialization phase, which is characterized by low network load and does not reflect steady-state or congested operating conditions.

Figure 3 illustrates the success probability, $P(\mathsf{S})$, as a function of the density of interfering UEs, across different values of B and T_{RA}. As expected, increasing the number of subcarriers from 12 to 48 significantly improves performance, allowing the system to support a density of $0.15 \cdot 10^{-2}$ to $0.7 \cdot 10^{-2}$ nodes per km^2 with $P(\mathsf{S})$ close to 1 when

[1]The MATLAB code will be made publicly available on GitHub upon completion of the revision process.

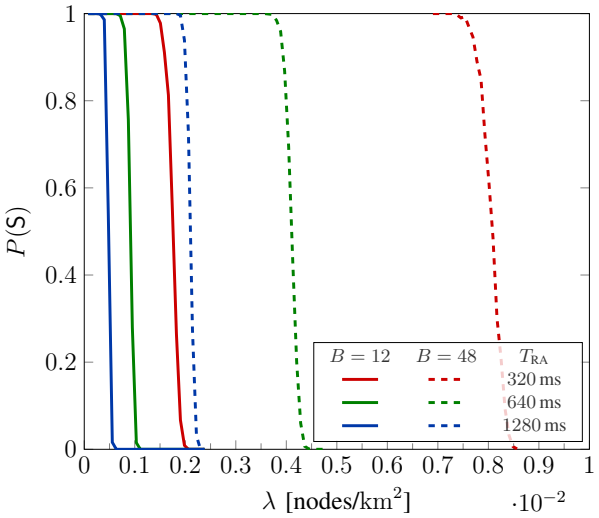

Fig. 3. Success probability as a function of the density of UEs, varying the RACH window periodicity and the number of subcarriers.

$T_{\mathrm{RA}} = 320$ ms. The figure shows that all curves exhibit a similar behavior, characterized by a very steep drop-off region. This sharp decline is likely due to congestion: as the number of users attempting transmission increases, the probability of successful transmission declines rapidly. This results in a quick transition from a stable operating state to one in which successful transmissions become increasingly rare. Furthermore, reducing the RACH window duration enhances the system's capacity to serve more devices, as this increases the number of effective RACH windows each device encounters during a satellite pass. However, shortening the RACH window duration also reduces the maximum payload that a device can transmit in a given RACH window. This trade-off implies that increasing the number of users that the system can accommodate may limit the payload each user can transmit to the satellite.

B. Analytical Model Validation

Let us now validate the analytical expression of the throughput derived in Section III by comparison with Monte Carlo simulations results. Figure 4 shows the simulated and analytical throughput of NB-IoT as a function of the number of backlogged users, with $B = 12$, varying the RACH window periodicity. The figure demonstrates that the analytical results closely match those of the simulations, thereby validating the proposed analytical framework. The figure also illustrates that maximum uplink throughput is achieved with $T_{\mathrm{RA}} = 320$ ms,

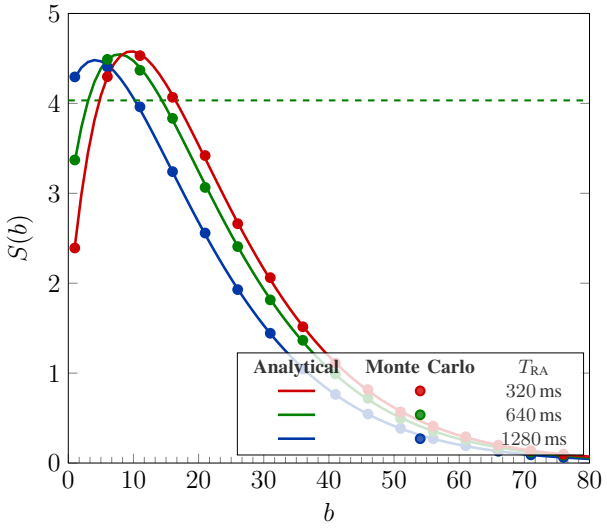

Fig. 4. Simulated and analytical throughput of NB-IoT as a function of the number of backlogged users b, with $B = 12$, varying the RACH window periodicity. The density of UEs is $\lambda = 10^{-3}$ [nodes/km^2]. The green dashed line shows the average number of packet arrivals at the satellite during a RACH window, $\bar{F}$, for $T_{\text{RA}} = 640$ ms.

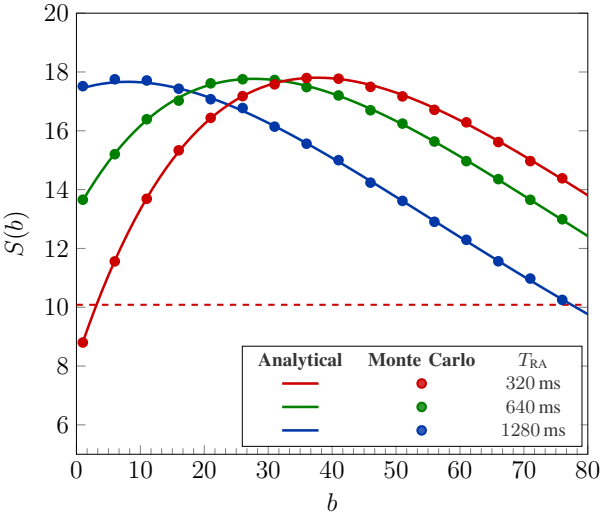

Fig. 5. Simulated and analytical throughput of NB-IoT with $B = 48$ varying the RACH window periodicity. The density of UEs is $\lambda = 5 \cdot 10^{-3}$ [nodes/km^2]. The red dashed line shows the average number of packet arrivals at the satellite, during a RACH window, $\bar{F}$, for $T_{\text{RA}} = 320$ ms.

which aligns with the results presented in Section IV-A. The green dashed lines in Figure 4 show the average number of fresh packet arrivals at the satellite during a RACH window, $\bar{F}$, for $T_{\text{RA}} = 640$ ms. The number of new arrivals within each RACH window follows a Poisson distribution, meaning that theoretically, the number of arrivals can be unbounded. This can lead to a situation where, as more users attempt to access the channel, the system becomes increasingly congested. In this congested state, only a small fraction of users successfully transmit, while a growing number of users experience collisions and become backlogged, shifting the system's operation towards the right side of the throughput curve, where it diminishes. However, when the density of the PPP is sufficiently low, the system is more likely to operate in a stable state for an extended period. In this stable condition, the system hovers around the first intersection point between the throughput curve and the dashed reference line, when it exists, where congestion remains minimal. This keeps the network operating efficiently, avoiding the drift toward a heavily backlogged state.

Figure 5 shows the simulated and analytical throughput of NB-IoT as a function of the number of backlogged users, with $B = 48$. Also in this case, the analytical results closely match those of the simulations, and the maximum uplink throughput is achieved with $T_{\text{RA}} = 320$ ms. Also here, the red dashed line shows the average number of fresh packet arrivals at the satellite during a RACH window, $\bar{F}$, for $T_{\text{RA}} = 320$ ms. It is evident how in case of $T_{\text{RA}} = 320$ ms there is an intersection between the dashed and the solid lines, identifying the operating point of the system.

ACKNOWLEDGEMENTS

Supported by the European Union under the Italian National Recovery and Resilience Plan of NextGenerationEU, partnership on "Telecommunications of the Future" (PE00000001 - "RESTART").

V. CONCLUSIONS

In conclusion, this study has explored the application of NB-IoT for DtS between IoT devices and LEO satellites, focusing on collision probability during the random access procedure and network throughput. Through an analytical model validated via simulations, we examined key NB-IoT protocol parameters in NTN contexts to highlight performance and deployment challenges. The results show how configuration choices, such as RACH window periodicity and subcarrier spacing, significantly impact network reliability and capacity, with important trade-offs between number of supported users and network throughput. These insights contribute to understanding the potential and limitations of using NB-IoT for IoT applications over NTN, providing a foundation for optimizing system configurations to meet global and remote connectivity needs.

REFERENCES

[1] O. Kodheli, N. Maturo, S. Chatzinotas, S. Andrenacci, and F. Zimmer, "NB-IoT via LEO satellites: An efficient resource allocation strategy for uplink data transmission," *IEEE Internet Things J.*, vol. 9, no. 7, pp. 5094–5107, 2022.

[2] M. Centenaro, C. E. Costa, F. Granelli, C. Sacchi, and L. Vangelista, "A survey on technologies, standards and open challenges in satellite IoT," *IEEE Commun. Surveys Tuts.*, vol. 23, no. 3, pp. 1693–1720, 2021.

[3] J. Jiao, S. Wu, R. Lu, and Q. Zhang, "Massive access in space-based Internet of Things: Challenges, opportunities, and future directions," *IEEE Wireless Commun.*, vol. 28, no. 5, pp. 118–125, Sep. 2021.

[4] S. K. Routray, R. Tengshe, A. Javali, S. Sarkar, L. Sharma, and A. D. Ghosh, "Satellite based IoT for mission critical applications," in *Proc. Int Conf. Data Science Commun.*, Bangalore, India, Mar. 2019.

[5] E. Testi and E. Paolini, "Packet collision probability analysis in contention-based direct-to-satellite IoT uplink," in *Proc. PIMRC 2024*, Valencia, Spain, Sep. 2024, pp. 1–6.

[6] ——, "Packet collision probability of direct-to-satellite IoT systems," *IEEE Internet Things J.*, vol. 12, no. 2, pp. 1843–1855, Sep. 2024.
[7] M. Asad Ullah, G. Pasolini, K. Mikhaylov, and H. Alves, "Understanding the Limits of LoRa Direct-to-Satellite: The Doppler Perspectives," *IEEE Open Journal of the Communications Society*, vol. 5, pp. 51–63, 2024.
[8] A. K. Dwivedi, S. Praneeth Chokkarapu, S. Chaudhari, and N. Varshney, "Performance analysis of novel direct access schemes for LEO satellites based IoT network," in *Proc. PIMRC 2020*, London, United Kingdom, Sep. 2020, pp. 1–6.
[9] Z. Qu, G. Zhang, H. Cao, and J. Xie, "LEO satellite constellation for Internet of Things," *IEEE Access*, vol. 5, pp. 18 391–18 401, 2017.
[10] C. Amatetti, M. Conti, A. Guidotti, and A. Vanelli-Coralli, "NB-IoT random access procedure via NTN: system level performances," in *ICC 2022*, Seoul, Korea, May 2022, pp. 2381–2386.
[11] G. Sciddurlo *et al.*, "Looking at NB-IoT Over LEO Satellite Systems: Design and Evaluation of a Service-Oriented Solution," *IEEE Internet of Things Journal*, vol. 9, no. 16, pp. 14 952–14 964, 2022.
[12] A. Petrosino *et al.*, "WIP: An open-source tool for evaluating system-level performance of nb-iot non-terrestrial networks," in *WoWMoM 2021*, Pisa, Italy, Jun. 2021, pp. 236–239.
[13] R. Marini, K. Mikhaylov, G. Pasolini, and C. Buratti, "Low-Power Wide-Area Networks: Comparison of LoRaWAN and NB-IoT Performance," *IEEE Internet of Things Journal*, vol. 9, no. 21, pp. 21 051–21 063, 2022.
[14] 3GPP, *TS 36.300 Group Radio Access Network. Evolved Universal Terrestrial Radio Access (E-UTRA) and Evolved Universal Terrestrial Radio Access Network (E-UTRAN). Overall description*, 2018.
[15] ——, *TS 36.213 LTE; Evolved Universal Terrestrial Radio Access (E-UTRA); Physical layer procedures*, 2020.
[16] ——, *TR 36.763; Study on Narrow-Band Internet of Things (NB-IoT) / enhanced Machine Type Communication (eMTC) support for Non-Terrestrial Networks*, 2021.